NeuroImage 60 (2012) 2096–2106

Contents lists available at SciVerse ScienceDirect

NeuroImage

journal homepage: www.elsevier.com/locate/ynimg

# On the use of correlation as a measure of network connectivity

Andrew Zalesky [a,*], Alex Fornito [a,b,c], Ed Bullmore [d,e]

[a] Melbourne Neuropsychiatry Centre, The University of Melbourne and Melbourne Health, Melbourne, Australia
[b] NICTA Victorian Research Laboratory, The University of Melbourne, Melbourne, Australia
[c] Centre for Neural Engineering, The University of Melbourne, Melbourne, Australia
[d] Behavioural and Clinical Neuroscience Institute, The University of Cambridge, Cambridge, UK
[e] Clinical Unit Cambridge, GlaxoSmithKline Cambridgeshire & Peterborough NHS Foundation Trust, Cambridge, UK

ARTICLE INFO

*Article history:*
Received 26 November 2011
Revised 31 January 2012
Accepted 3 February 2012
Available online 11 February 2012

*Keywords:*
Brain connectivity
Connectome
Small-world network
Correlation
Partial correlation
Transitivity

ABSTRACT

Numerous studies have demonstrated that brain networks derived from neuroimaging data have nontrivial topological features, such as small-world organization, modular structure and highly connected hubs. In these studies, the extent of connectivity between pairs of brain regions has often been measured using some form of statistical correlation. This article demonstrates that correlation as a measure of connectivity in and of itself gives rise to networks with non-random topological features. In particular, networks in which connectivity is measured using correlation are inherently more clustered than random networks, and as such are more likely to be small-world networks. Partial correlation as a measure of connectivity also gives rise to networks with non-random topological features. Partial correlation networks are inherently less clustered than random networks. Network measures in correlation networks should be benchmarked against null networks that respect the topological structure induced by correlation measurements. Prevalently used random rewiring algorithms do not yield appropriate null networks for some network measures. Null networks are proposed to explicitly normalize for the inherent topological structure found in correlation networks, resulting in more conservative estimates of small-world organization. A number of steps may be needed to normalize each network measure individually and control for distinct features (e.g. degree distribution). The main conclusion of this article is that correlation can and should be used to measure connectivity, however appropriate null networks should be used to benchmark network measures in correlation networks.



## Introduction

Recent years have witnessed a surge of interest in mapping and modeling the complicated web of connectivity that comprises the brain, termed the connectome. Large-scale brain networks have been central to this work (Bullmore and Sporns, 2009; Habeck and Moeller, 2011; He and Evans, 2010; Kaiser, 2011; Wig et al., 2011). They consist of a network of brain regions together with a measure of connectivity between every possible pair of these regions (Rubinov and Sporns, 2011).

In functional brain networks, connectivity is often measured using some form of statistical correlation. The brain activity at one region is correlated with the activity at another to quantify the strength and sign of any statistical dependency. When repeated for every possible pair of regions, the result is a network characterization of the brain's connectivity, where brain regions represent network nodes and correlation strengths correspond to connection weights.

Numerous studies have demonstrated functional brain networks have various nontrivial topological features, such as small-world organization, modular structure and highly connected hubs (Achard et al., 2006; Bassett and Bullmore, 2006; Hayasaka and Laurienti, 2010; Telesford et al., 2010; van den Heuvel and Hulshoff Pol, 2010; van den Heuvel et al., 2008). However, the interpretation of the small-world concept as well as other topological measures derived from path length is not straightforward in functional networks. This is because functional networks are intrinsically fully connected, and thus the "path length" between a pair of regions is already explicitly captured by the strength of correlation in brain activity; namely, the weight of the direct connection (Rubinov and Sporns, 2010).

The purpose of this article is to draw attention to the pitfalls of probing brain networks for small-world properties. Networks are said to be small-world if they are substantially more clustered than random networks, yet have approximately the same characteristic path length as random networks (Watts and Strogatz, 1998). This article begins by showing that networks in which connectivity is measured using correlation can inherently satisfy the two criteria required of small-world networks (Section 2). In particular, the use of correlation as a measure of connectivity *in and of itself* gives rise

* Corresponding author.
*E-mail address:* azalesky@unimelb.edu.au (A. Zalesky).

1053-8119/$ – see front matter © 2012 Elsevier Inc. All rights reserved.
doi:10.1016/j.neuroimage.2012.02.001

to networks that are inherently more clustered than random networks, and as such are more likely to be small-world networks.

A similar observation was recently reported (Bialonski et al., 2011), where the length and spectral content of multivariate electroencephalographic recordings were found to influence topological structure. The main contributions of this article are to provide an explanation for this observation, namely *why* correlation networks have a propensity to be small-world networks (Section 3), as well as to present strategies for generating null networks to normalize for the inherent topological structure induced by correlation measurements (Section 4). Related null networks have been generated using Markov chain (Bansal et al., 2009) and generative models (Volz, 2004).

In Section 3, evidence is presented suggesting that although strong positive correlation between $X$ and $Y$ as well as $Y$ and $Z$ theoretically does not imply strong positive correlation between $X$ and $Z$ (Langford et al., 2001), in functional brain networks, this *is* the case. In particular, strong positive correlation on the indirect path ($X$-$Y$-$Z$) implies correlation on the direct connection ($X$-$Z$) that is significantly greater than expected in random networks (although this does not mean that indirect paths necessarily predict direct connections in all instances). This effect is referred to as *transitivity* and is used to explain why correlation networks are inherently more clustered than random networks.

In Section 4, null networks are presented to normalize for the inherent topological structure found in correlation networks, resulting in more conservative estimates of small-world organization. Traditionally, normalization has been performed with respect to randomly rewired networks matched for degree distribution (Maslov and Sneppen, 2002). This kind of topology randomization is shown to overestimate the degree to which brain networks are small-world networks.

Whenever we refer to *correlation networks* in this article, we mean *any* kind of network in which connectivity is measured using the correlation coefficient. While we focus on functional brain networks, our conclusions and methods also apply to metabolite, protein and gene correlation networks (Gillis and Pavlidis, 2011; Junker and Schreiber, 2008), financial portfolio networks (Hirschberger et al., 2004) and anatomical brain networks in which connectivity is measured using correlation in cortical thickness or volume (Bassett et al., 2008; He et al., 2007).

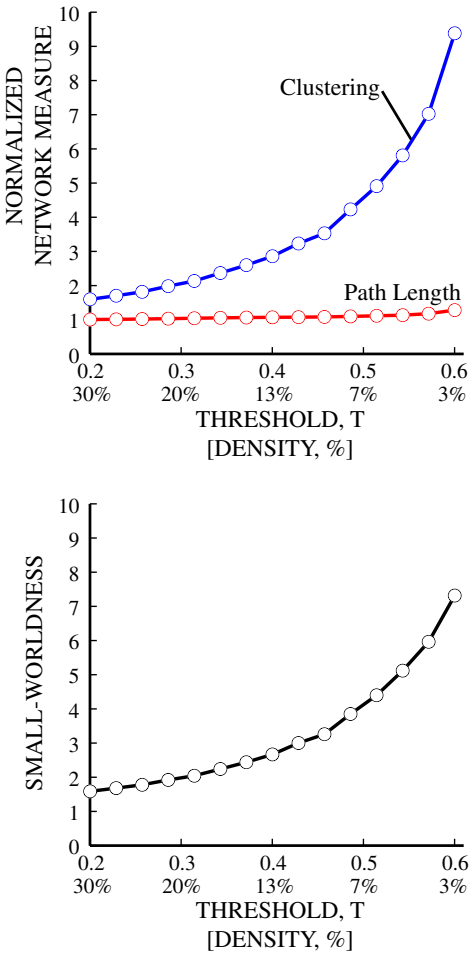


**Fig. 1.** Small-world organization of correlation networks generated by correlating independent white noise ($N = 90$). Correlation values exceeding a threshold of $T$ were set to unity, indicating a network connection, while all other values were set to zero. The ratio between the correlation network's clustering coefficient and the clustering coefficient of its randomized version is plotted in blue (normalized clustering coefficient). The ratio between its characteristic path length and the characteristic path length of its randomized version is plotted in red (normalized path length). The ratio between the normalized clustering coefficient and the normalized path length is plotted in black (summary statistic of small-worldness). The horizontal axis shows the threshold, $T$, and directly below, the connection density corresponding to this threshold.

## Correlation induces small-world organization

A set of $N$ random vectors were generated. Vectors comprised $n$ elements, each independently sampled from a normal distribution of zero mean and unity variance. The correlation between every possible pair of vectors was calculated, yielding an $N \times N$ random correlation matrix with values ranging between -1 and 1 (Holmes, 1991). Vectors were generated independent of each other to ensure no interdependence. Non-random topological structure evident in the correlation matrix was therefore a matter of chance alone.

The random correlation matrix was viewed as the connectivity matrix for a hypothetical brain network with $N$ nodes. Values exceeding a threshold of $T$ were set to unity, indicating presence of a connection, while all other values were set to zero (Rubinov and Sporns, 2010). This process of "binarizing" a connectivity matrix based on a fixed threshold is a well-established practice and has been implemented in the majority of studies investigating the small-world organization of brain networks (Ginestet et al., 2011; van Wijk et al., 2010). The clustering coefficient and characteristic path length (harmonic mean) (Watts and Strogatz, 1998) were then calculated. The network was randomly rewired (Maslov and Sneppen, 2002) and these two measures were recalculated for the randomized version of the network. The average over an ensemble of 20 randomizations was used. Given that the network was random to begin with, the clustering coefficient and characteristic path length presumably should not significantly differ between the original network and its randomized version.

Surprisingly, this was not the case. Fig. 1 shows the ratio between the clustering coefficient of the original network and the clustering coefficient of its randomized version (blue). This ratio is also shown for the characteristic path length (red). Fig. 1 also shows the ratio of these two ratios (black), which serves as a commonly used summary statistic of small-worldness (Humpheries and Gurney, 2008). The network is a small-world network on all accounts. It is substantially more clustered than its randomized version (ratio $\gg 1$), yet its characteristic path length is only slightly greater (ratio $\approx 1$).

The expectation was that all three ratios would have been approximately unity, which would have indicated against any non-random topological structure. This is clearly not the case. How is it possible for a random correlation matrix to result in a network that is unequivocally a (non-random) small-world network?

The reason is that random correlation matrices are not random matrices. In particular, the transitive nature of the correlation coefficient induces non-random topological structure that would not be expected in random networks matched for network size and degree distribution. The implication of this observation is that correlation networks are inherently more clustered than random networks, and as such are more likely to be small-world networks.

The number of nodes, $N$, was set to 90, a value common to many previous studies (Zalesky et al., 2010). The effect was exactly

replicated for values of $N$ up to 1000. Values exceeding 1000 were not investigated for computational reasons.

The number of elements, $n$, comprising each random vector was set to 10. The effect was replicated for $n = 64$, 128, 256, 512 as well as for random vectors that were simulated with the Black-Scholes model and fractional Gaussian noise. The Black-Scholes model has been used to simulate financial correlation networks (Vertes et al., 2011), while fractional Gaussian noise with a Hurst parameter exceeding 0.5 has been suggested as a potential model for the functional-MRI BOLD signal (Maxim et al., 2005). The volatility and drift rate for the Black-Scholes model were set based on real financial data (Vertes et al., 2011). Fractional Gaussian noise with a Hurst parameter of 0.9 and unity variance was used. Fig. 2 shows the normalized clustering coefficient (blue) and the normalized

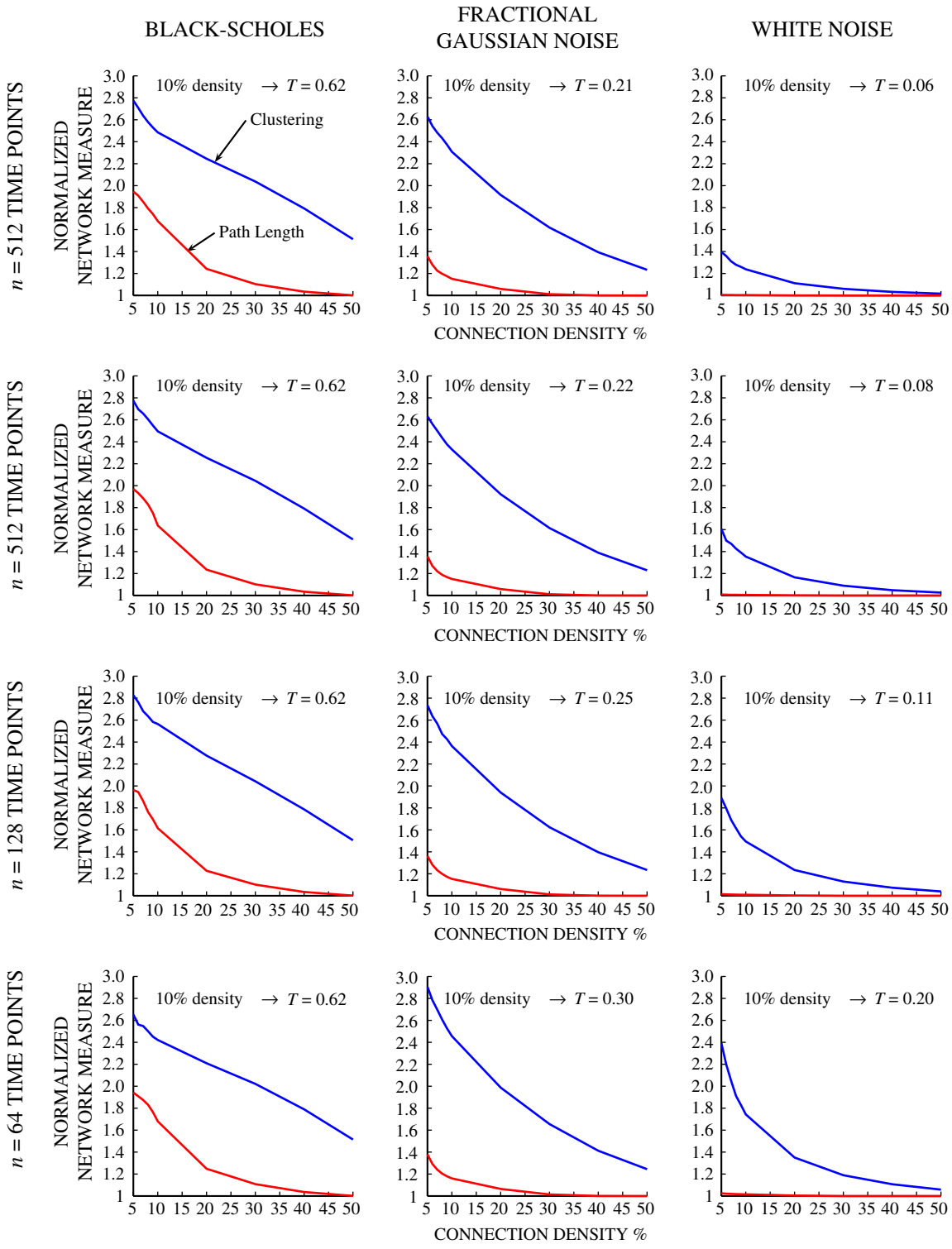


**Fig. 2.** Small-world properties of correlation networks generated by correlating $N = 90$ independent time series of length $n = 64, 128, 256, 512$. Time series were simulated with the Black-Scholes model, fractional Gaussian noise with a Hurst parameter of 0.9 and white noise. The normalized clustering coefficient is plotted in blue and the normalized characteristic path length is plotted in red. The binarizing threshold, $T$, used to achieve a nominal connection density of 10% is indicated for each case.

characteristic path length (red) for $n=64$, 128, 256, 512 (rows in Fig. 2) and for random times series simulated with the Black-Scholes model, fractional Gaussian noise and white noise (columns in Fig. 2). Normalization was once again with respect to the average over an ensemble of 20 randomized versions of the original correlation network (Maslov and Sneppen, 2002).

Fig. 2 demonstrates that correlating fractional Gaussian noise as well as time series simulated with the Black-Scholes model give rise to networks that are also inherently more clustered than random networks, with minimal dependence on the value of $n$. However, in the case of white noise, the clustering effect begins to diminish as the value of $n$ is increased. This is because correlating white noise gives rise to correlation values that tend to become more narrowly distributed about zero as $n$ is increased. Of the three models, fractional Gaussian noise is the most relevant to this study because it is the most realistic model for the BOLD signal.

In Fig. 2, the thresholds used to binarize the correlation matrices generated with the Black-Scholes model and fractional Gaussian noise were representative of the thresholds typically applied to actual functional-MRI correlation matrices. For example, to achieve a nominal connection density of 10%, a binarizing threshold of 0.62 was used for the Black-Scholes model (irrespective of $n$) and thresholds of 0.30 ($n=64$), 0.25 ($n=128$), 0.22 ($n=256$) and 0.21 ($n=512$) were used for fractional Gaussian noise. However, in the case of white noise, lower thresholds were needed because correlating white noise gives rise to correlation values that tend to become more narrowly distributed about zero as $n$ is increased. In particular, to achieve a nominal connection density of 10% for the white noise case, binarizing thresholds of 0.20 ($n=64$), 0.11 ($n=128$), 0.08 ($n=256$) and 0.06 ($n=512$) were used.

The effect was evident over a range of connection densities. The connection density is the ratio between the number of actual connections, denoted $E$, and the total possible number of connections, $N(N-1)/2$. In the literature, small-world organization has been examined over a very diverse range of connection densities. Densities as low as 1-5% (e.g. Achard et al., 2006; Kitzbichler et al., 2011) and as high as 50% (e.g. Lynall et al., 2011) have been considered. The minimum connection density for which small-world organization has been estimated has often been chosen to satisfy $k>log(N)$, where $k$ is the mean nodal degree (Achard et al., 2006). This rule yields a minimum connection density of 5% when $N=90$.

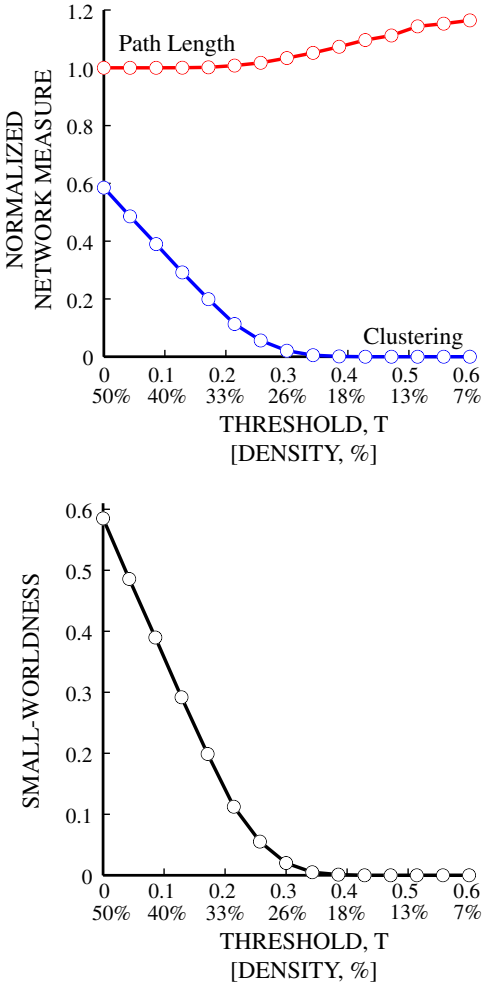


**Fig. 3.** Small-world organization of random *partial* correlation matrices ($N=90$). Normalized clustering coefficient shown in blue, normalized characteristic path length shown in red and the ratio of the two shown in black.

*Partial Correlation*

Partial correlation is a different measure of functional (Salvador et al., 2005) and anatomical (Bassett et al., 2008) connectivity that has received recent interest (Marrelec et al., 2009). With partial correlation, the brain activity at one region is correlated with the activity at another, with the activity at all other *N-2* regions regressed out. Partial correlation attempts to remove the effect of indirect paths (Smith et al., 2011). However, partial correlation is only suitable for cases in which $n>N$.

Does measurement of functional connectivity using partial correlation also induce non-random topological features? To answer this question, the experiment performed above was repeated using partial correlation. Once again, a set of $N$ random vectors were generated independently. The correlation between every possible pair of vectors was calculated, but this time regressing out the *N-2* remaining vectors to yield partial correlation coefficients.

Fig. 3 is the equivalent of Fig. 1 for the case of partial correlation. Using partial correlation resulted in networks inherently less clustered than random networks (ratio $\ll 1$).

*Summary*

Using correlation to measure connectivity in and of itself gives rise to networks with non-random topological features.

- Full correlation networks are inherently more clustered than random networks. Full correlation networks are therefore more likely to be small-world networks. (With the exception of Black-Scholes correlation networks, which additionally display a considerably greater characteristic path length than random networks.)
- Partial correlation networks are inherently less clustered than random networks.

Network measures are benchmarked against random networks that do not respect the inherent topological structure of correlation networks. Consequently, the extent of small-world organization may be overestimated with full correlation and underestimated with partial correlation.

## Indirect paths predict direct connections

It has been shown that correlation networks are inherently more clustered than random networks, and as such are more likely to be small-world networks. In this section, an attempt is made to elucidate *why* this is the case.

The clustering coefficient can be defined in terms of triangles and triples. A *triangle* of node $i$ is a subgraph comprising three nodes, one of which is $i$, and three connections. A *triple* of node $i$ is a subgraph comprising three nodes, one of which is $i$, and two connections,

both of which are connected to $i$. The clustering coefficient is then given by

$$C_i = \frac{\{\text{triangles of node } i\}}{\{\text{triples of node } i\}}.$$

The denominator is fixed by the degree of node $i$; namely, $k(k-1)/2$, where $k$ is the degree. This leaves the number of triangles as the only free variable determining the clustering coefficient. As such, the greater the proportion of triangles, the higher the clustering coefficient

Triangles of node $i$ can be thought of in terms of an indirect path spanning two connections, $u$-$i$-$v$, and a direct connection, $u$-$v$. Triples on the other hand consist of only an indirect path (Fig. 4). From this viewpoint, the greater the proportion of direct connections, the greater the clustering coefficient. More specifically, high clustering requires that the presence of an indirect path, $u$-$i$-$v$, is associated with the presence of a direct connection, $u$-$v$.

Indirect paths need not share any association with direct connections in general networks. However, this is not the case for networks in which connectivity is measured using correlation. In correlation networks, a lower bound can be derived for the correlation of the direct connection, $\rho_{u,v}$, in terms of the correlation of the two connections comprising the indirect path, $\rho_{u,i}$ and $\rho_{i,v}$; namely,

$$\begin{aligned}\rho_{u,v} &= cos\left(\theta_{u,v}\right) \geq cos\left(\theta_{u,i} + \theta_{i,v}\right)\\ &= cos\left(\theta_{u,i}\right)cos\left(\theta_{i,v}\right) - sin\left(\theta_{u,i}\right)sin\left(\theta_{i,v}\right)\\ &= \rho_{u,i}\rho_{i,v} - \sqrt{1-\rho_{u,i}^2}\sqrt{1-\rho_{i,v}^2},\end{aligned}$$

where the time series for each node is regarded as an $n$-dimensional vector and $\theta_{u,v}$ denotes the angle formed between the zero-mean centered vectors for nodes $u$ and $v$. This lower bound has been derived in detail elsewhere (Langford et al., 2001) and discussed in the context of gene networks (Gillis and Pavlidis, 2011). It has also been suggested as evidence against an association between indirect paths and direct connections (Erhardt et al., 2011). For example, the bound asserts that $\rho_{u,v}$ need only be greater than zero if $\rho_{u,i} = \rho_{i,v} = 0.7$. Nevertheless, it must be remembered that this is merely a theoretical bound, which in practice might not be tight.

To determine the extent of the association between indirect paths and direct connections *in practice*, the following experiment was undertaken. Every possible combination of three nodes, each called a *triad*, was enumerated in a random correlation network. For a network of 90 nodes, this was $\binom{90}{3} = 117480$ triads. Triads were partitioned into two mutually exclusive groups: positive triads and negative triads. Positive triads contained at least two connections with positive correlation values, while negative triads contained at least two connections with negative correlation values.

The indirect path and direct connection was then determined for each positive triad. The direct connection was defined as the connection with the lowest correlation value, leaving the remaining two connections to form the indirect path.

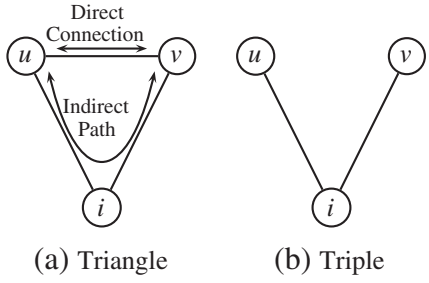


**Fig. 4.** A triangle and a triple of node $i$.

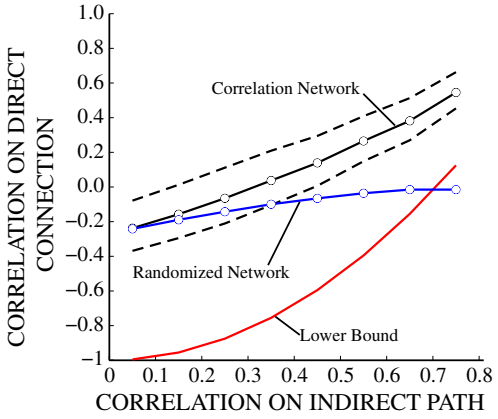


**Fig. 5.** Correlation on the direct connection, $\rho_{direct}$, as a function of correlation on the indirect path, $\rho_{indirect}$, shown for a random correlation network, its randomized version and the theoretical lower bound.

The correlation value on the direct connection was plotted as a function of the correlation value on the indirect path (Fig. 5). Each positive triad contributed a single data point to this plot. The correlation value on the indirect path, denoted $\rho_{indirect}$, was conservatively chosen as the minimum of its two correlation values; namely, $\rho_{indirect} = min(\rho_{u,i}, \rho_{i,v})$. The correlation value on the direct connection, $\rho_{direct}$, was unambiguous.

For the sake of plot clarity, the horizontal axis was stratified into bins of length 0.1 and the data points within each bin were averaged. The dashed lines in Fig. 5 indicate the 25th and 75th percentiles, while the solid line (black) indicates the mean. The lower bound was also plotted on the same axes (red), based on substitution of $\rho_{u,i}$ and $\rho_{i,v}$ with $\rho_{indirect}$.

To evaluate whether the association between indirect paths and direct connections was greater than expected in random networks, the experiment was repeated using a randomized version of the original correlation network. Given that the original correlation network was a random correlation network to begin with, this randomization served only to annihilate any topological structure incurred due to the transitive nature of the correlation coefficient.

Fig. 5 suggests the lower bound is not tight in practice. For example, when $\rho_{indirect} = 0.7$, the bound asserts $\rho_{direct}$ can in principle be as low as 0. However, Fig. 5 shows that $\rho_{direct} = 0.5$ when $\rho_{indirect} = 0.7$. Therefore, in correlation networks, high values of $\rho_{indirect}$ predict high values of $\rho_{direct}$. Indeed, Fig. 5 shows this association is considerably stronger than expected in random networks. In random networks, $\rho_{direct} = -0.1$ when $\rho_{indirect} = 0.7$.

The consequence of this result is that correlation networks are inherently predisposed to contain a greater proportion of triangles compared to networks in which connectivity is not measured using correlation, such as connectivity inferred from axonal fiber tracking. This is because the use of correlation makes it more likely that the presence of an indirect path is associated with the presence of the corresponding direct connection. When the indirect path and corresponding direct connection are both present, a triangle is formed. Given that the clustering coefficient is dictated by the proportion of triangles, it follows that correlation networks are inherently more clustered than random networks.

The propensity for the formation of triangles has been referred to as triadic closure in the literature on social network theory (Granovetter, 1973). In social networks, triadic closure occurs because if Alice and Bob are both associated with Jill, the opportunity for Alice and Bob to meet and create at least a weak association is increased through their mutual friendship with Jill. It is important to note that this kind of "social" triadic closure is a topological property that is *intrinsic* to social networks. In contrast, the increased triadic closure found in correlation networks is a result of the transitive nature of the correlation coefficient. This should not be misinterpreted as a "problem" with using the correlation coefficient as a measure of connectivity. It is rather a "problem"

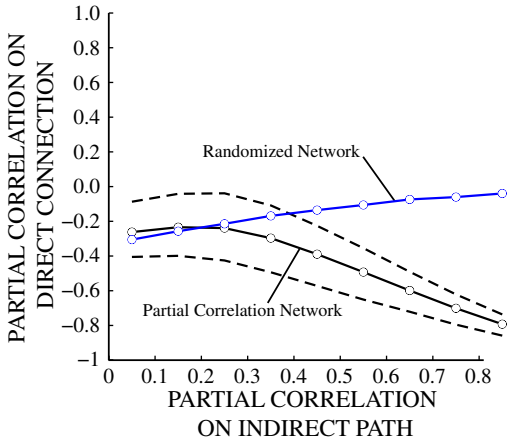


**Fig. 6.** Partial correlation on the direct connection, $\rho_{direct}$, as a function of correlation on the indirect path, $\rho_{indirect}$, shown for a random correlation network and its randomized version.

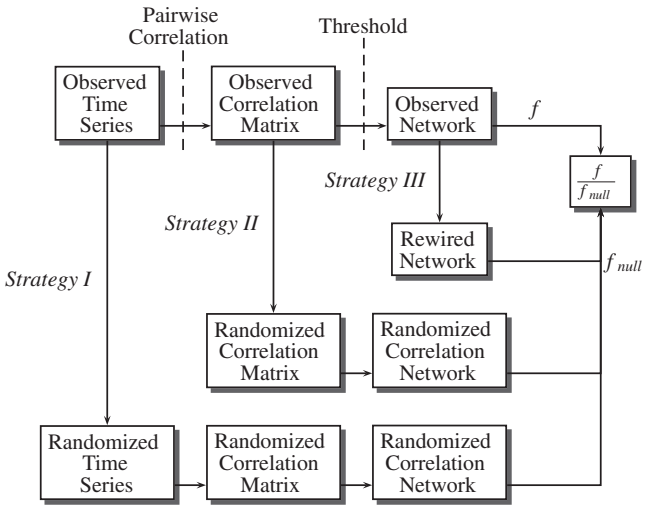


**Fig. 7.** Strategies for generating null networks. Strategy I: time series randomization. Strategy II: correlation matrix randomization. Strategy III: topology randomization (e.g. random rewiring). $f$ denotes the network measure calculated for the observed network, while $f_{null}$ denotes the same network measure averaged over the ensemble of null networks.

with the fact that correlation networks are benchmarked against null networks (i.e. random networks) that do not preserve the transitive structure of correlation networks.

Fig. 6 is the equivalent of Fig. 5 for the case of partial correlation. The lower bound is not shown because it does not apply to partial correlation. In partial correlation networks, high values of $\rho_{indirect}$ predict low (negative) values of $\rho_{direct}$, more so than expected in random networks. This is consistent with the fact that partial correlation networks are inherently less clustered than random networks.

## Normalization

Networks are customarily benchmarked against an ensemble of null networks to quantify the extent to which topological properties such as small-world organization are expressed. Topology randomization is the most widely used strategy for generating null networks, and is typically performed by randomly rewiring the observed network (Maslov and Sneppen, 2002).

This kind of random rewiring not only annihilates intrinsic topological structure in the empirical data, it also annihilates topological structure induced by correlation transitivity, referred to as *transitive structure*. The random rewiring algorithm cannot distinguish intrinsic topological structure from transitive structure, and thus they are both annihilated. Ideally, it is only intrinsic structure that should be annihilated during randomization, whereas transitive structure should be preserved.

To understand this, let $f/f_{null}$ denote a given normalized network measure, where $f$ is the network measure calculated for the observed network and $f_{null}$ is the same network measure averaged over an ensemble of null networks. In practice, the experimenter is interested only in quantifying intrinsic network structure expressed in the empirical data. The difficulty is that $f$ captures both intrinsic and transitive structure. Therefore, the normalization term, $f_{null}$, should capture transitive structure so that when the ratio $f/f_{null}$ is taken, transitive structure is canceled out. In other words, normalization of network measures should respect the transitive structure of correlation networks.

This indicates the need for null networks that preserve transitive structure. Two distinct strategies are proposed to generate such null networks (Fig. 7): time series randomization (Strategy I) and correlation matrix randomization (Strategy II). These two strategies are demonstrated to yield more conservative estimates of small-world organization compared to the more widely used strategy of topology randomization (Strategy III).

### *Correlation matrix randomization*

Correlation matrix randomization involves generating null networks from randomly generated correlation matrices. The same processing steps applied to the observed correlation matrix are applied to each randomly generated null correlation matrix, resulting in an ensemble of null networks.

Null correlation matrices can be generated by correlating a set of random vectors (Holmes, 1991). However, the distribution of correlation values that results is not necessarily matched to the observed distribution of correlation values. Therefore, applying the same threshold to both the observed and null correlation matrices can yield networks that are not matched in terms of connection density.

To avoid this, we consider algorithms to randomly generate null correlation matrices that are matched to the distribution of observed correlation values. This yields null networks that are simultaneously matched in terms of connection density and threshold.

The Hirschberger-Qi-Steuer (H-Q-S) algorithm (Hirschberger et al., 2004) randomly generates null covariance matrices that are matched to the distributional properties of an observed covariance matrix. The algorithm was originally devised to generate realistic covariance matrices for financial applications related to portfolio optimization. Working in terms of covariance matrices is not a restriction because covariance matrices can be transformed to correlation matrices by normalizing with respect to standard deviations. The H-Q-S algorithm matches the mean and variance of the off-diagonal elements (covariances) as well as the mean of the diagonal elements (variances). Higher order moments can also be matched, however, this can lead to numerical instability.

To confirm the validity of the H-Q-S algorithm, a new algorithm was developed for randomly generating null correlation matrices with a desired mean and variance. The new algorithm adopts a brute-force approach, which is appreciably slower than the H-Q-S algorithm, but yields a more accurately matched distribution of correlation values. The H-Q-S algorithm and the new brute-force matching algorithm are described in the Appendix, where an evaluation of their accuracy is also presented.

### *Time series randomization*

Time series randomization involves randomizing the observed time series by taking its Fourier transform, scrambling its phase and then inverting the transform (Prichard and Theiler, 1994). It can also be performed using wavelet techniques (Breakspear et al., 2004). The autocorrelation function, power spectrum and other linear properties are preserved under phase scrambling.

The difficulty with time series randomization is that the correlation matrices that result are not necessarily matched to the

distribution of observed correlation values. Therefore, different thresholds may need to be used to ensure the null networks are matched in terms of connection density.

The same scrambling sequence can be applied to each time series to preserve the distribution of correlation values (Prichard and Theiler, 1994), but in this case, only the nonlinear properties are randomized. To randomize linear correlations as well, the phase of each time series was scrambled using a different scrambling sequence.

Matching in terms of connection density was always given precedence over matching in terms of threshold.

*Results*

An established resting-state functional-MRI data preprocessing protocol (Achard et al., 2006; Bullmore and Sporns, 2009) was applied to map functional brain networks ($N=90$) in 10 healthy individuals. Correction for the global mean signal remains controversial and was not performed.

No spatial smoothing was performed as part of the preprocessing protocol. However, functional-MRI data inherently comprises some degree of spatial smoothing due to the acquisition process. This inherent spatial smoothing can produce specious short-range connections that in turn inflate the clustering coefficient in high-resolution networks where individual voxels represent distinct nodes (e.g. van den Heuvel et al., 2008; Zalesky et al., in press). This effect is less of a concern for the coarse networks analyzed here because the size of each node greatly exceeds the spatial extent of the smoothing range.

Moreover, it is important to note that the inherent clustering arising from the transitive nature of the correlation coefficient is a distinct phenomenon from the clustering induced by spatial smoothing. Spatial smoothing is an idiosyncrasy specific to functional-MRI, whereas the clustering induced by transitivity is pertinent to all types of correlation networks; for example, gene networks, financial portfolio networks and anatomical brain networks derived from correlation in cortical thickness.

The small-world properties of the functional brain networks were benchmarked against null networks generated using three different randomization strategies: time series randomization, correlation matrix randomization and topology randomization.

Fig. 8 shows the distribution of correlation values for an arbitrary individual (black line). The distributions of five null correlation matrices generated with time series randomization (5 dashed blue lines) and five null correlation matrices generated with correlation matrix randomization (5 dashed red lines) are also shown on the same axes. Correlation matrix randomization closely follows the distribution of observed correlation values, enabling matching in terms of both connection density and threshold.

Fig. 9 shows the ratio $f/f_{null}$ averaged over the 10 networks, where $f$ denotes the clustering coefficient (top) and the characteristic path length (middle). Fig. 9 also shows the ratio of these two ratios (bottom), which serves as a summary statistic of small-worldness. Correlation matrix randomization was performed with both the H-Q-S algorithm (red line) and the brute-force mean/variance matching algorithm (blue line). Fig. 10 shows the corresponding "raw" measures; namely, $f$ and $f_{null}$ separately.

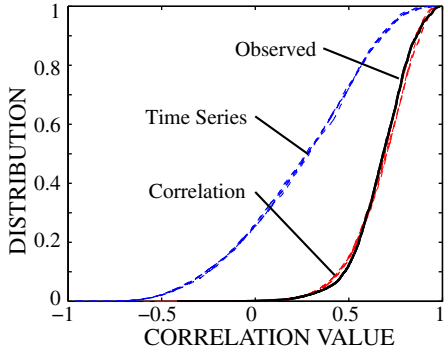


**Fig. 8.** Cumulative distribution function of correlation values for an arbitrary individual (black line) compared to the distributions of five null correlation matrices generated with time series randomization (5 dashed blue lines) and five null correlation matrices generated with correlation matrix randomization (5 dashed red lines).

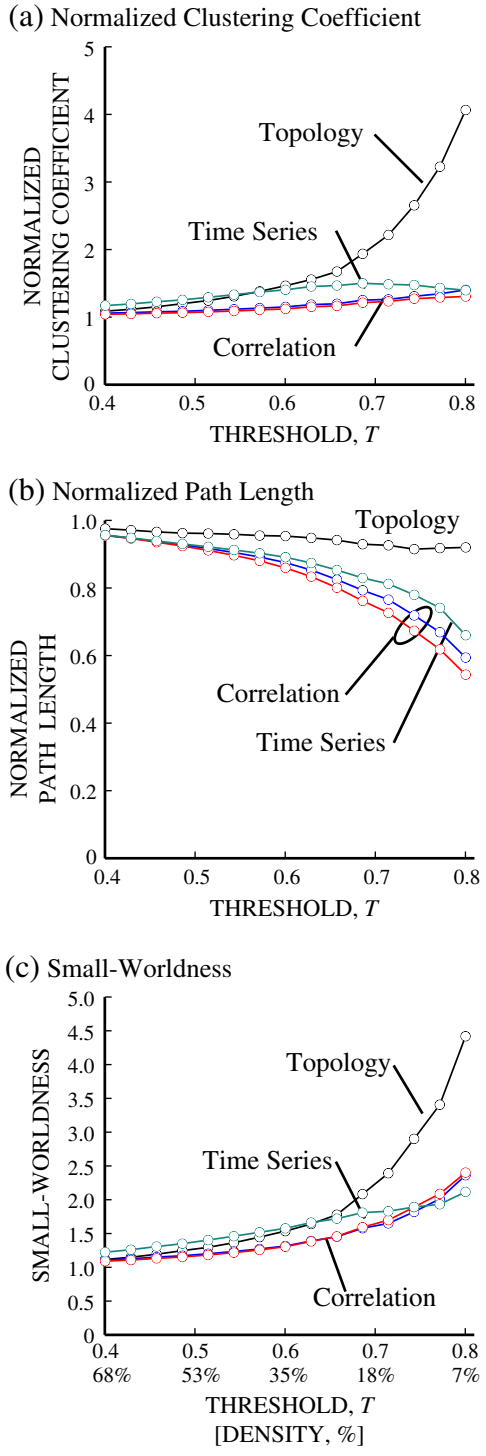


**Fig. 9.** Small-world organization quantified with null networks generated using three different randomization strategies: time series randomization (time series), correlation matrix randomization (correlation) and topology randomization (topology). For correlation matrix randomization, the H-Q-S algorithm (red line) and a brute-force mean-variance algorithm (blue line) were used to generate the null networks.

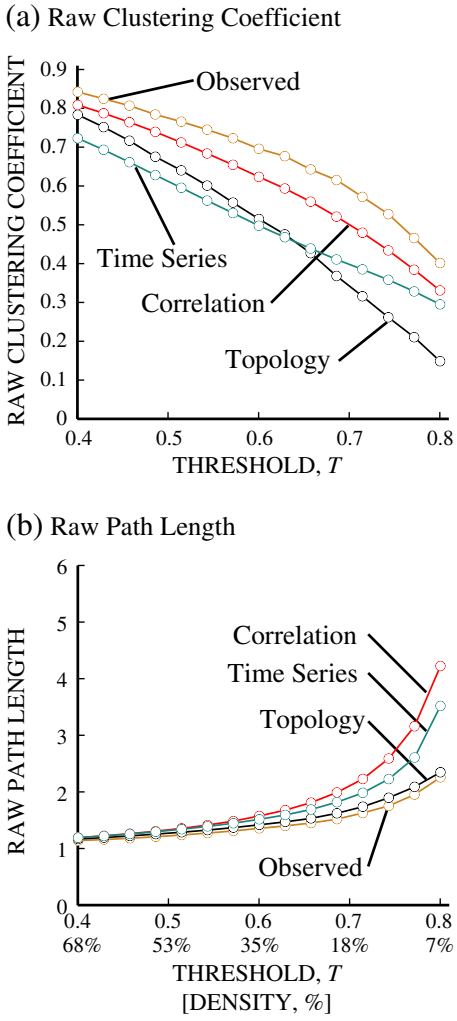


**Fig. 10.** Raw clustering coefficient and raw path length measured in null networks generated using three different randomization strategies: time series randomization (time series), correlation matrix randomization (correlation) and topology randomization (topology). Correlation matrix randomization was performed with the H-Q-S algorithm.

Correlation matrix randomization and time series randomization behaved similarly, with both strategies exhibiting comparable trends. Topology randomization behaved quite differently though.

For the threshold of $T = 0.8$ (density $\approx 7\%$), the observed clustering coefficient was more than four times greater than the null networks generated with topology randomization, but only 1.5 times greater than the null networks generated with correlation matrix randomization. This equates to a discrepancy of approximately 60% between topology and correlation matrix randomization in their estimates of the normalized clustering coefficient.

The observed characteristic path length was about the same as the null networks generated with topology randomization (ratio $\approx 1$), but shorter than the null networks generated with correlation matrix randomization (ratio $< 1$). This can be explained by the fact that the null networks generated with correlation matrix randomization are matched only in terms of mean degree, which gives rise to a uniform degree distribution. In contrast, matching in terms of degree distribution preserves high degree hub nodes, which are conducive to shorter path lengths.

Generating a null network that preserves the nodal degree distribution may be considered critical for the purposes of path length normalization. If this is the case, one approach is to normalize the characteristic path length with topology randomization and normalize the clustering coefficient with correlation matrix randomization. This ensures high degree hubs nodes are preserved for normalization of the characteristic path length. Modifying the null network to suit specific network measures has recently been suggested in Telesford et al. (2011), where the clustering coefficient was normalized with respect to an equivalent lattice network.

The agreement between the H-Q-S algorithm (red line) and the brute-force mean/variance matching algorithm (blue line) was excellent. In the case of the clustering coefficient and the summary statistic of small-worldness, the agreement was too great to allow clear distinction between the red and blue plots. This indicates the choice of algorithm for generating null correlation matrices is immaterial. The H-Q-S algorithm should be used in practice on the grounds of computational speed.

### *Summary*

Networks are benchmarked against appropriate null networks to quantify the extent to which topological properties such as small-world organization are evident. Null networks have been traditionally derived via topological reorganization of the observed network in a random fashion. For example, a popular approach is to randomly rewire the observed network, while preserving its degree distribution. The extent to which correlation networks are small-world networks can be overestimated if benchmarking is relative to null networks derived in this manner because the inherent transitive structure of correlation networks is not respected. Randomization of correlation networks should instead be performed at the correlation matrix level by randomly generating null correlation matrices that are matched in distribution to the observed correlation matrix. Time series randomization is another suitable strategy, although it requires the use of different thresholds to ensure matching of connection densities.

The main limitation of time series and correlation matrix randomization is that only the mean nodal degree can be matched, but not the degree distribution. This can result in longer path lengths due to the randomization of hub nodes.

## Conclusion

Networks express pairwise relationships between sets of objects. Implicit to network analysis is that the mere measurement of these pairwise relations is topologically neutral. That is, measurement performed between one pair of objects does not affect measurements performed on other pairs in such a way that produces non-random topological structure.

This is not the case for networks measured using correlation or partial correlation. The use of correlation as a measure of connectivity gives rise to networks that are inherently more clustered than random networks, and as such are more likely to be small-world networks. This is due to the transitive nature of the correlation coefficient, which effectively means indirect paths and their corresponding direct connections are more likely to coexist in correlation networks compared to random networks.

This should not be thought of as a “problem” with the correlation coefficient as a measure of connectivity per se, but rather a “problem” with the fact that experimenters benchmark correlation networks against null networks that do not preserve the inherent topological features found in correlation networks. The main contribution of this article was to propose null networks that explicitly normalize for the inherent topological structure found in correlation networks. This resulted in a more conservative estimate of small-world organization.

Rather than using null networks that normalize for the transitivity inherent to correlation networks, an alternative is to directly eliminate “false” transitive closures in the observed correlation network once it has been computed. This is achieved with heuristic criteria, such as triangle reduction (Rice et al., 2005) or transitive reduction (Klamt et al., 2010), which seek to systematically eliminate direct connections that can be potentially explained by indirect paths.

Another alternative is to eliminate "false" transitive closures simply by eliminating every triangle (Ramsey et al., 2011), although this will invariably yield a clustering coefficient of zero.

As a reviewer of this work has rightfully pointed out, the transitive nature of the correlation coefficient may also have a bearing on the interpretation, normalization and validity of other important network measures, such as modularity, efficiency, centrality and motif counts (Rubinov and Sporns, 2010). While the focus of this study has been on the two most common measures of characteristic path length and the clustering coefficient, more work is needed to assess any impact on other network measures. More work is also needed to extrapolate our results to other types of correlation networks, such as metabolite, protein and gene networks as well as financial portfolio networks.

## Acknowledgments

A.Z. is grateful for the support provided by Professor Trevor Kilpatrick as part of the inaugural Melbourne Neuroscience Institute Fellowship. This work was also supported by the Australian Research Council [DP0986320 to A.Z.]; the Melbourne Neuroscience Institute; and the National Health and Medical Research Council of Australia [C.J. Martin Fellowship to A.F. ID: 454797]. We are grateful to Dr Mikail Rubinov for reviewing the first draft of this manuscript and for providing many fruitful suggestions.

## Appendix

This appendix presents two algorithms for randomly generating null correlation matrices with specified distributional properties. A.1 presents the H-Q-S algorithm, A.2 presents the brute-force mean/variance matching algorithm. A.3 provides a numerical evaluation of these two algorithms.

### *A.1. Hirschberger-Qi-Steuer Algorithm*

The H-Q-S algorithm randomly generates null covariance matrices. The algorithm is based on Cholesky decomposition, which asserts that for any matrix $\mathbf{X}\in\mathbb{R}^{N\times m}$, the matrix $\mathbf{X}\mathbf{X}^T$ is positive semi-definite, and can thus function as a covariance matrix. The basic idea is to independently sample the elements of $\mathbf{X}$ from a Gaussian distribution. The mean, $\mu$, and variance, $\sigma^2$, of this Gaussian distribution as well as the value of $m$ are chosen to ensure the distributional properties of the null covariance matrix $\mathbf{X}\mathbf{X}^T$ are matched to the observed covariance matrix. The observed covariance matrix is characterized in terms of the mean, $e$, and variance, $v$, of its off-diagonal elements (covariances) as well as the mean, $\bar{e}$, of its diagonal elements (variances). This is referred to as the $ev-\bar{e}$ mode of the algorithm. Other modes are available in which higher order moments are matched. Pseudocode for the $ev-\bar{e}$ mode of H-Q-S algorithm is shown in Algorithm 1. The covariance matrix, $\mathbf{C}$, can be transformed to a correlation matrix using $\mathbf{aCa}$, where $\mathbf{a}=\mathrm{diag}\left(1/\sqrt{\mathbf{C}_{1,1}},\ldots,1/\sqrt{\mathbf{C}_{N,N}}\right)$.

**Algorithm 1**. Hirschberger-Qi-Steuer

Generate a null covariance matrix, $\mathbf{C}\in\mathbb{R}^{N\times N}$, with mean $e$ and variance $v$ for the off-diagonal elements (covariances), and mean $\bar{e}$ for the diagonal elements (variances).

**inputs** $e$, $v$, $\bar{e}$ and $N$
$m\leftarrow max(2,\lfloor(\bar{e}^2-e^2)/v\rfloor)$
$\mu\leftarrow\sqrt{e/m}$
$\sigma^2\leftarrow-\mu^2+\sqrt{\mu^4+v/m}$
$x_{i,j}\sim\mathcal{N}(\mu,\sigma^2)$, $i=1,\ldots,N$ $j=1,\ldots,m$
$\mathbf{X}=(x_{i,j})_{i=1,\ldots,N;\,j=1,\ldots,m}$
$\mathbf{C}=\mathbf{X}\mathbf{X}^T$
**return C**

### *A.2. Brute-Force Mean/Variance Matching Algorithm.*

A new algorithm is provided to randomly generate null correlation matrices with the distribution of correlation values matching a given mean, $\mu$, and variance, $\sigma^2$. Let $\mathbf{X}=(\mathbf{x}_1,\ldots,\mathbf{x}_N)$ be $N$ independent random vectors, where $\mathbf{x}=(x_1,\ldots,x_n)^T\sim\mathcal{N}(0,\mathbf{I})$. Without loss of generality, assume $\mathbb{E}(\mathbf{x})=0$ and $\|\mathbf{x}\|=1$, then the Gram matrix,

$$\rho=\mathbf{X}\mathbf{X}^T\in[-1,1]^{N\times N}$$

is a random correlation matrix with mean given by $\hat{\mu}=\sum_{i=1}^{N}\sum_{j=i+1}^{N}\rho_{i,j}/c$ and variance given by $\hat{\sigma}^2=\sum_{i=1}^{N}\sum_{j=i+1}^{N}\left(\rho_{i,j}-\hat{\mu}\right)^2/c$, where $c=N(N-1)/2$.

The objective is to choose $\mathbf{X}$ such that $\hat{\mu}=\mu$ and $\hat{\sigma}^2=\sigma^2$. To this end, consider: i) adjusting $\hat{\sigma}^2$ via the dimension of $\mathbf{x}$, denoted $n$; and, ii) adjusting $\hat{\mu}$ via a common random vector $\mathbf{y}=(y_1,\ldots,y_n)^T\sim\mathcal{N}(0,\mathbf{I})$, which is added to each of $\mathbf{x}_1,\ldots,\mathbf{x}_N$; namely,

$$\mathbf{x}_i\leftarrow\mathbf{x}_i+a\mathbf{y},\quad i=1,\ldots,N, \tag{1}$$

where $a\geq0$. Although no proof is given, we have noted empirically that $\hat{\sigma}^2$ is monotonically decreasing with $n$ and $\hat{\mu}$ is monotonically increasing with $a$. A binary search can therefore be performed on $a$ to determine the value of $a$ giving $\hat{\mu}\approx\mu$, followed by another binary search performed on $n$ to determine the value of $n$ giving $\hat{\sigma}^2\approx\sigma^2$.

Pseudocode is shown in Algorithm 2, where the upper terminals of the binary search, $\alpha$ and $\beta$, are chosen sufficiently large to encompass the desired mean and variance. Extensive numerical testing suggests algorithm convergence as long as $\mu$ and $\sigma^2$ are chosen within reasonable limits.

**Algorithm 2**. Brute-Force Mean/Variance Matching

Generate a null correlation matrix, $\rho\in[-1,1]^{N\times N}$, with mean $\mu$ and variance $\sigma^2$.

**inputs** $\mu$, $\sigma^2$ and $N$
$n_{max}=\alpha$; $n_{min}=2$
**while** $n_{max}-n_{min}>1$ **do**
  $n\leftarrow\lfloor n_{min}+(n_{max}-n_{min})/2\rfloor$
  $\rho=\texttt{fit\_mean}(n,\mu)$
  $\hat{\mu}\leftarrow\sum_{i=1}^{N}\sum_{j=i+1}^{N}\rho_{i,j}/c$
  $\hat{\sigma}^2\leftarrow\sum_{i=1}^{N}\sum_{j=i+1}^{N}\left(\rho_{i,j}-\hat{\mu}\right)^2/c$
  **if** $\hat{\sigma}^2>\sigma^2$ **then**
    $n_{min}\leftarrow n$
  **else**
    $n_{max}\leftarrow n$
  **end if**
**end while**
**return** $\rho$

fit_mean
Generate a null correlation matrix, $\rho\in[-1,1]^{N\times N}$, with mean $\mu$.
**inputs** $\mu$, $n$ and $N$
$\mathbf{x}_i=(x_1,\ldots,x_n)^T\sim\mathcal{N}(0,\mathbf{I}),\ i=1,\ldots,N$
$\mathbf{y}=(y_1,\ldots,y_n)^T\sim\mathcal{N}(0,\mathbf{I})$
$a_{max}=\beta$; $a_{min}=0$
**while** $|a_{max}-a_{min}|>0.001$ **do**
  $a\leftarrow a_{min}+(a_{max}-a_{min})/2$
  $\mathbf{x}_i\leftarrow\mathbf{x}_i+a\mathbf{y}$, $i=1,\ldots,N$
  Normalize so that $\mathbb{E}(\mathbf{x}_i)=0$ and $\|\mathbf{x}_i\|=1$
  $\rho\leftarrow\mathbf{X}\mathbf{X}^T$, where $\mathbf{X}=(\mathbf{x}_1,\ldots,\mathbf{x}_N)$
  $\hat{\mu}\leftarrow\sum_{i=1}^{N}\sum_{j=i+1}^{N}\rho_{i,j}/c$
  **if** $\hat{\mu}>\mu$ **then**
    $a_{max}\leftarrow a$
  **else**
    $a_{min}\leftarrow a$
  **end if**
**end while**

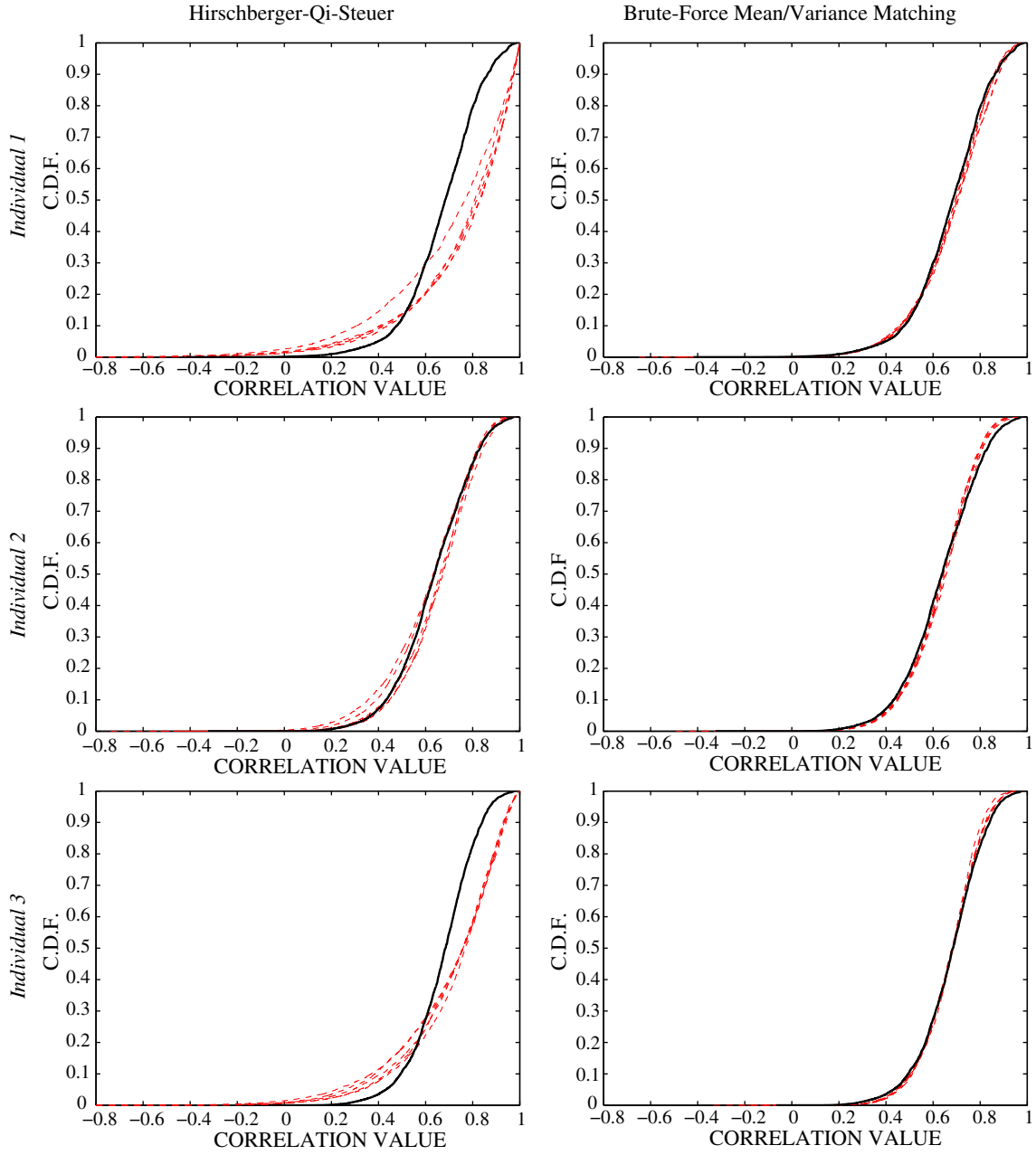


**Fig. 11.** Cumulative distribution function (CDF) for five null correlation matrices (5 dashed red lines) and the observed correlation matrix (solid black line). The three leftmost axes correspond to the H-Q-S algorithm, while the three rightmost axes correspond to the brute-force mean/variance matching algorithm.

### *A.3. Numerical Evaluation*

The H-Q-S algorithm and the brute-force mean/variance algorithm were evaluated using covariance matrices derived from three of the individuals considered in Section 4. A total of five null correlation matrices were randomly generated for each individual using each of the two algorithms (5 null correlation matrices per individual per algorithm). To evaluate how well the distribution of the null correlation values matched the distribution of the observed correlation values, the cumulative distribution function (CDF) was plotted on the same axes for each of the five null correlation matrices (5 dashed red lines) as well as the observed correlation matrix (solid black line). Fig. 11 shows the CDFs segregated according to algorithm and individual. The brute-force mean/variance algorithm yielded a better match for all three individuals. The H-Q-S algorithm also yielded satisfactory results. A null correlation matrix can be generated in less than one second with the H-Q-S algorithm, whereas the brute-force algorithm requires about one minute.

## References

Achard, S., Salvador, R., Whitcher, B., Suckling, J., Bullmore, E., 2006. A resilient, low-frequency, small-world human brain functional network with highly connected association cortical hubs. J. Neurosci. 26 (1), 63–72.
Bansal, S., Khandelwal, S., Meyers, L.A., 2009. Exploring biological network structure with clustered random networks. BMC Bioinformatics 10, 405.
Bassett, D.S., Bullmore, E., 2006. Small-world brain networks. Neuroscientist 12 (6), 512–523.
Bassett, D.S., Bullmore, E., Verchinski, B.A., Mattay, V.S., Weinberger, D.R., Meyer-Lindenberg, A., 2008. Hierarchical organization of human cortical networks in health and schizophrenia. J. Neurosci. 28 (37), 9239–9248.
Bialonski, S., Wendler, M., Lehnertz, K., 2011. Unraveling spurious properties of interaction networks with tailored random networks. PLoS One 6 (8), e22826.
Breakspear, M., Brammer, M.J., Bullmore, E.T., Das, P., Williams, L.M., 2004. Spatiotemporal wavelet resampling for functional neuroimaging data. Hum. Brain Mapp. 23, 1–25.

Bullmore, E.T., Sporns, O., 2009. Complex brain networks: graph-theoretical analysis of structural and functional systems. Nat. Rev. Neurosci. 10, 186–198.
Erhardt, E.B., Allen, E.A., Damaraju, E., Calhoun, V.D., 2011. On network derivation, classification, and visualization: a response to Habeck and Moeller. Brain Connect 1 (2), 1–19.
Gillis, J., Pavlidis, P., 2011. The role of indirect connections in gene networks in predicting function. Bioinformatics 27 (13), 1860–1866.
Ginestet, C.E., Nichols, T.E., Bullmore, E.T., Simmons, A., 2011. Brain network analysis: separating cost from topology using cost-integration. PLoS One 6 (7), e21570.
Granovetter, M., 1973. The strength of weak ties. Am. J. Sociol. 78 (6), 1360–1380.
Habeck, C., Moeller, J.R., 2011. Intrinsic functional-connectivity networks for diagnosis: just beautiful pictures? Brain Connect. 1 (2), 99–103.
Hayasaka, S., Laurienti, P.J., 2010. Comparison of characteristics between region-and voxel-based network analyses in resting-state fMRI data. Neuroimage 50 (2), 499–508.
He, Y., Evans, A., 2010. Graph theoretical modeling of brain connectivity. Curr. Opin. Neurol. 23 (4), 341–350.
He, Y., Chen, Z.J., Evans, A.C., 2007. Small-world anatomical networks in the human brain revealed by cortical thickness from MRI. Cereb. Cortex 17 (10), 2407–2419.
Hirschberger, M., Qi, Y., Steuer, R.E., 2004. Randomly generating portfolio-selection covariance matrices with specified distributional characteristics. Eur. J. Oper. Res. 177 (3), 1610–1625.
Holmes, R.B., 1991. On random correlation matrices. Siam J. Matrix Anal. Appl. 12 (2), 239–272.
Humpheries, M.D., Gurney, K., 2008. Network 'small-world-ness': a quantitative method for determining canonical network equivalence. PLoS One 3, e0002051.
Junker, B.H., Schreiber, F., 2008. Analysis of Biological Networks. Wiley-Interscience. (ISBN-10: 0470041447).
Kaiser, M., 2011. A tutorial in connectome analysis: topological and spatial features of brain networks. Neuroimage 57, 892–907.
Kitzbichler, M.G., Henson, R.N., Smith, M.L., Nathan, P.J., Bullmore, E.T., 2011. Cognitive effort drives workspace configuration of human brain functional networks. J. Neurosci. 31 (22), 8259–8270.
Klamt, S., Flassig, R.J., Sundmacher, K., 2010. TRANSWESD: inferring cellular networks with transitive reduction. Bioinformatics 26 (17), 2160–2168.
Langford, E., Schwertman, N., Owens, M., 2001. Is the property of being positively correlated transitive? Am. Stat. 55 (4), 322–325.
Lynall, M.-E., Bassett, D.S., Kerwin, R., McKenna, P.J., Kitzbichler, M., Muller, U., Bullmore, E., 2011. Functional connectivity and brain networks in schizophrenia. J. Neurosci. 30 (28), 9477–9487.
Marrelec, G., Kim, J., Doyon, J., Horwitz, B., 2009. Large-scale neural model validation of partial correlation analysis for effective connectivity investigation in functional MRI. Hum. Brain Mapp. 30 (3), 941–950.
Maslov, S., Sneppen, K., 2002. Specificity and stability in topology of protein networks. Science 296, 910–913.
Maxim, V., Sendur, L., Fadili, J., Suckling, J., Gould, R., Howard, R., Bullmore, E., 2005. Fractional Gaussian noise, functional MRI and Alzheimer's disease. Neuroimage 25 (1), 141–158.
Prichard, D., Theiler, J., 1994. Generating surrogate data for time series with several simultaneously measured variables. Phys. Rev. Lett. 73 (7), 951–954.
Ramsey, J.D., Hanson, S.J., Glymour, C., 2011. Multi-subject search correctly identifies causal connections and most causal directions in the DCM models of the Smith et al. simulation study. Neuroimage 58 (3), 838–848.
Rice, J.J., Tu, Y., Stolovitzky, G., 2005. Reconstructing biological networks using conditional correlation analysis. Bioinformatics 21 (6), 765–773.
Rubinov, M., Sporns, O., 2010. Complex network measures of brain connectivity: uses and interpretation. Neuroimage 52 (3), 1059–1069.
Rubinov, M., Sporns, O., 2011. Weight-conserving characterization of complex functional brain networks. Neuroimage 56 (4), 2068–2079.
Salvador, R., Suckling, J., Coleman, M.R., Pickard, J.D., Menon, D., Bullmore, E., 2005. Neurophysiological architecture of functional magnetic resonance images of human brain. Cereb. Cortex 15 (9), 1332–1342.
Smith, S.M., Miller, K.L., Salimi-Khorshidi, G., Webster, M., Beckmann, C.F., Nichols, T.E., Ramsey, J.D., Woolrich, M.W., 2011. Network modelling methods for FMRI. Neuroimage. 54, 875–891.
Telesford, Q.K., Morgan, A.R., Hayasaka, S., Simpson, S.L., Barret, W., Kraft, R.A., Mozolic, J.L., Laurienti, P.J., 2010. Reproducibility of graph metrics in FMRI networks. Front. Neuroinf. 4, 117.
Telesford, Q.K., Joyce, K.E., Hayasaka, S., Burdette, J.H., Laurienti, P.J., 2011. The ubiquity of small-world networks. Brain Connect. 1 (5), 367–375.
van den Heuvel, M.P., Hulshoff Pol, H.E., 2010. Exploring the brain network: a review on resting-state fMRI functional connectivity. Eur. Neuropsychopharmacol. 20 (8), 519–534.
van den Heuvel, M.P., Stam, C.J., Boersma, M., Hulshoff Pol, H.E., 2008. Small-world and scale-free organization of voxel-based resting-state functional connectivity in the human brain. Neuroimage 3 (3), 528–539.
van Wijk, B.C.M., Stam, C.J., Daffertshofer, A., 2010. Comparing brain networks of different size and connectivity density using graph theory. PLoS One 5 (10), e13701.
Vertes, P.E., Nicol, R.M., Chapman, S.C., Watkins, N.W., Robertson, D.A., Bullmore, E.T., 2011. Topological isomorphisms of human brain and financial market networks. Front. Syst. Neurosci. 5, 75.
Volz, E., 2004. Random networks with tunable degree distribution and clustering. Phys. Rev. E 70 (4), 056115.
Watts, D.J., Strogatz, S.H., 1998. Collective dynamics of 'small-world' networks. Nature 393, 440–442.
Wig, G.S., Schlaggar, B.L., Petersen, S.E., 2011. Concepts and principles in the analysis of brain networks. Ann. N. Y. Acad. Sci. 1224 (1), 126–146.
Zalesky, A., Fornito, A., Harding, I.H., Cocchi, L., Yucel, M., Pantelis, C., Bullmore, E.T., 2010. Whole-brain anatomical networks: does the choice of nodes matter? Neuroimage 50 (3), 970–983.
Zalesky, A., Fornito, A., Egan, G.F., Pantelis, C., Bullmore, E.T., in press. The relationship between regional and inter-regional functional connectivity deficits in schizophrenia. Hum. Brain Mapp. doi:10.1002/hbm.21379.